Engineering Science & Technology
http://ojs.wiserpub.com/index.php/EST/

UNIVERSAL WISER PUBLISHER

Research Article

The Numerical Simulation and Performance Analysis of Seawater Desalination Unit: The Case of SWRO Station with Energy Recovery Devices (ERDs)

Ahmed Ghadhy*, Amine Lilane, Abdelkader Boulezhar, Dennoun Saifaoui

Laboratory of Renewable Energies and Systems Dynamics, Faculty of Sciences Ain-Cock, University of Hassan II, Casablanca, Morocco
E-mail: ahmedghadhy2018@gmail.com

Received: 24 August 2024; **Revised:** 27 November 2024; **Accepted:** 9 December 2024

Abstract: The demand for good quality drinking water is experiencing strong growth on a global scale, particularly in emerging countries, such as the BASIC countries (Brazil, South Africa, India, and China). For this reason, sea water or brackish water desalination technology using membrane filtration technique is a very effective and sustainable method for dealing with this problem. In this work, the performance study of the reverse osmosis desalination plant of Nouadhibou, Mauritania, coupled or not with an energy recovery unit, was carried out using the Matlab/Simulink software. The objective of this work is to study the functional and productive performance of the reverse osmosis unit by examining the importance of the pressure exchanger in such systems and the impact on the mixing rate of feed water with the flow of water delivered by the pressure exchanger. This study shows that the exploited Energy Recovery Devices (ERDs) provide highly favorable economic and energetic profitability, with a 75% reduction in energy consumption. Specifically, the specific power consumption is reduced from 14.5 kWh/m^3 to 5 kWh/m^3 when ERDs are used, for a productivity of 800 m^3/d and a recovery rate of 20%.

***Keywords*:** reverse osmosis, seawater, energy recovery, specific power consumption, desalination

Nomenclature

A	Area, m^2
BF	Backing factor, %
C_p	Specific heat capacity, J/kg·°C, at constant pressure
FF	Fill factor, %
HPP	High-pressure pump, kW
LF	Load factor, %
M	Mass flow rate, m^3/h, kg/s
N, n	Number, -
P	Power, kW, or Pressure, bar
PEX	Pressure exchanger
ppm	Parts per million

DOI: https://doi.org/10.37256/est.6120255559

RO	Reverse Osmosis
RR	Recovery ratio
SPC	Specific power consumption, kWh/m^3
SR	Salt rejection
T	Temperature, °C
k	Permeability
X	Salinity ratio, g/kg (ppm)
Y	Extraction percentage, %

Subscripts

a	Ambient
av	Average
b	Brine
bp	Booster pump
d	Distillate product, discharge
e	Element
f	Feed
h	High
i	Inlet
o	Outlet
p	Product or pump
th	Thermal
total	Total
s	Salt
spl	Splitted
w	Water
PEX	Pressure exchanger

Greek symbol

Δ	Difference
η	Efficiency, %
η_{PEX}	Pressure exchanger splitter ratio
$\eta_{f,\,PEX}$	Pressure exchanger efficiency
ρ	Density, kg/m^3
Π	Osmotic pressure, kPa

1. Introduction

With the population growth and industry development, the water needs increase, we talk about an increase of 50% in Africa, 25% in Asia, 14% in the USA, and 2% in Europe [1] within the century. On the other hand, 1.2 billion people haven't access to potable water every year, and 3,900 children die every day because of polluted water [1]. However, water covers almost three-quarters of the planet's surface, about 97.5% of the earth's water is salt from the oceans, and only 2.5% of freshwater from groundwater, lakes, and rivers, provide most of human and animal needs [2].

Nowadays, more than 47 m^3 millions of potable water are produced per day in more than 15,000 desalination plants [3]. Desalination has proved to be the best solution for the freshwater scarcity challenge, by separating freshwater from saline water [4]-[6]. There are two categories of desalination processes: thermal process and membrane-based process. The thermal process is based on the evaporation and condensation of the water. This process includes three technologies: multi-stage flash (MSF), multi-effect distillation (MED), and vapor compression (VC). The membrane-

based process separates the water molecules from the saline feed water by a semi-permeable membrane [7]. The electrical consumption of sea water reverse osmosis (SWRO), MSF, and MED is 3-6 kWh/m^3, 4-6 kWh/m^3, 1.5-2.5 kWh/m^3, respectively [8]-[11].

Reverse osmosis, due to its high efficiency, simple equipment, and convenient maintenance [12]-[16], has become the predominant technology among all desalination processes, accounting for 65% of the market share [17], [18]. A reverse osmosis desalination system involves several stages: pretreatment, where raw water is cleaned and disinfected [19]-[21]; a high-pressure pump that forces pre-treated water through RO membranes; pressure vessels containing RO membranes that filter water, removing salts and impurities; energy recovery devices that reduce energy consumption by reusing the brine pressure; post-treatment to adjust the water's pH, minerals, and overall quality; and finally, storage and distribution, where the purified water is stored and delivered to users [22]-[24]. Eshoul et al. [25] conducted an exergy analysis of a two-pass reverse osmosis (RO) desalination system with a capacity of 127 m^3/h. His findings show that the use of Energy Recovery Turbine (ERT) and Pressure Exchanger (PEX) technologies resulted in a reduction of the overall energy consumption of the desalination process by about 30% and 50%, respectively. Additionally, the specific power consumption (SPC in kWh/m^3) decreased from 7.2 kW/m^3 to 5.0 kW/m^3 with ERT, and to 3.6 kW/m^3 with Pressure Exchanger (PEX). The energy efficiency of the RO desalination process improved by 49% with ERT and by 77% with PEX, while exergy destruction was reduced by 40% for ERT and by 53% for PEX. Wang et al. [26] conducted a performance comparison between the ERT and PEX systems at a desalination plant located on an island in China. The results revealed that the effective energy conversion efficiency (EECE) of the PEX ERD was 93.9%, which is 15.5% higher than that of the turbine energy recovery device (ERD). Additionally, the specific power consumption (SPC) of the PEX ERD was 3.03 kWh/m^3, slightly lower than the turbine ERD by approximately 0.34 kWh/m^3. T. M. Mansour et al. [27] conducted a study to determine the effectiveness of a pressure exchanger (PEX) used in a 2.4 m^3/d reverse osmosis (RO) unit. The results showed that the PEX reduced power consumption by 80%.

This work is the first of its kind to conduct a performance study of an energy recovery device, PEX, at a desalination plant in Mauritania, thereby demonstrating the effectiveness of this device while also examining other parameters. The purpose of this paper is to study the performance of the Nouadhibou SWRO plant without the energy recovery devices (ERDs) of pressure exchanger (PEX) type under different parameters (see Figure 1) to investigate the energy benefit that could give PEX to a SWRO unit and the performances of the unit with and without PEX. We will study the variation in the production of the station (m^3/h) as a function of the inlet pressure, the variation in the salinity of the permeate as a function of the inlet pressure and the salinity of the feed water, and we will calculate the different specific energy consumptions (SEC). These simulations will be carried out on a model designed using MATLAB software. Next, we will compare these data from the station without ERDs with the real data from the station with ERDs, to see the differences and the advantages of the implementation of energy recovery devices and their influence on the SEC. We will discuss the results in both cases, and we will interpret them then we will end with a conclusion that will include the main keywords and the main results of this study.

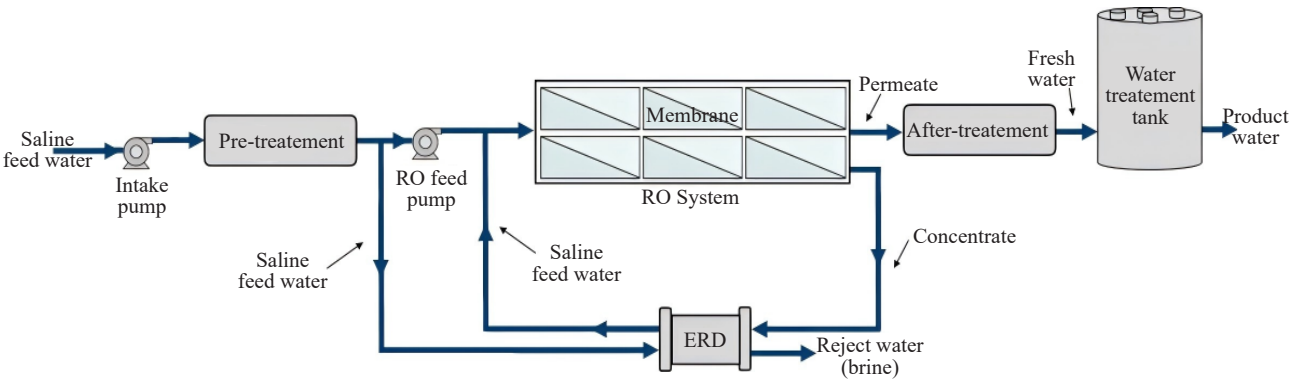

Figure 1. Schema of a SWRO plant in all steps

2. Energy recovery devices

In a reverse osmosis system, an important portion of feed flux, the concentrate, is rejected by the membrane with high pressure. So, this hydraulic energy can be recovered through an energy recovery device ERD. The first design performed at the beginning of 1980 used systems based on a centrifugal pump, an engine, and either, Francis or Pelton hydraulic turbines. These systems give SECs less than 5 kWh/m^3 [25]-[30].

The energy recovery devices are classified into two categories: isobaric ERDs and centrifugal ERDs. The earliest centrifugal ERDs include the Pelton turbine, turbocharger, and reverse centrifugal pump. The centrifugal ERD transforms the concentrated energy into mechanical energy to drive the pump. These devices had a maximum net transfer efficiency of less than 70% at their best efficiency point [31].

Since around the year 2000, isobaric ERDs have replaced centrifugal ERDs in most new SWRO stations. Isobaric ERDs transform the brine energy directly into the feed flux, where the feed flux and the brine come into direct contact (with minimal mixing). Consequently, efficiency losses are reduced and that is why these devices are more efficient than centrifugal ERDs [32], [33]. There are two main types of isobaric ERDs: rotary-type pressure exchangers and piston-type work exchangers:

- The pressure exchanger: The pressure exchanger (PEX) uses the principle of positive displacement to allow raw water to be pressurized directly by contact with the brine left under pressure from the membrane module. It uses a cylindrical rotor with channels longitudinal and parallel to its axis of rotation to transfer pressure from the discharge to the raw water. It rotates between two fixed nozzles with inlet and outlet ports for low and high pressure [34].

- The work exchangers: in which the transfer of energy between concentrate and feed stream occurs inside hydraulic cylinders, with the alternating pressurization/depressurization process controlled by a switcher valve [33]. Work exchanger ERDs are less compact and modular than pressure exchanger devices and require higher capital outlay and maintenance due to the need for control actuators and valves [31].

These isobaric ERDs have an operating efficiency of up to 98% [35]. The isobaric ERDs are mainly used in large-scale SWRO plants and although the flow of a single device is low, parallel units are used [36]. Centrifugal ERDs are used in small SWRO plants with large single flow rates and stable operation. The specific energy consumption (SEC), kWh/m^3, which is the ratio of power consumed to the permeate flow, is an important parameter of the RO system performance and plays an important role in system energy consumption. It is also related to the recovery efficiency of ERDs [37], [38].

The energy analysis of reverse osmosis systems working on different scales with and without energy recovery devices (ERDs) shows that their energy consumption can be significantly decreased by coupling ERDs [39], [40]. The isobaric ERD can give an SEC reduction of up to 60% while the centrifugal ERD gives an SEC reduction of 45%. The use of ERDs has decreased the SEC in SWRO and BWRO systems to less than 3 kWh/m^3 and 1 kWh/m^3, respectively [41].

3. Description of the studied plant

In Mauritania, the north of Africa, only 68% of the population had access to water in 2016, which represents a quantity of 50 liters per person per day. The rural zones suffer from water scarcity due to a shortage of rainfall [42]. The issue is that in some areas with dense populations, water sources are scarce. Even though the water is extracted from underground, it is brackish [43]. The country produces 600 million m^3 for different goals: agriculture, mines, and water supply [42], [43]. The water resources are classed into two categories: surface water and underground water. Consequently, the desalination capacity in the country can reach 5,000 m^3 per day [43].

In the north of Nouadhibou country at coordinates 20.9425° N, 17.0362° W, people also suffer from water shortages [44]. The city has about 118,000 inhabitants. The seawater reverse osmosis desalination plant in Nouadhibou was built near the sea, located close to the Cansado Falls. It is the only desalination station directed by the National Water Society (Société Nationale des Eaux, SNDE) in the country. Completed in 2019, the plant supplies water to the city of Cansado in the southern part of Nouadhibou. The project of this plant was to go through a first phase offering a supply of drinking water to the city of Nouadhibou by 5,000 m^3 per day, and then in the second phase, this capacity will be

increased to 15,000 m^3 per day. The total cost of the project was 630 million Ouguiyas MRU, which was entirely borne by the Mauritanian state budget. Actually, the plant produces 3,000 m^3/day of freshwater.

Figure 2. (a) Multi-media filtration units, (b) Cartridge filters, (c) Clean-in-place (CIP) system, (d) Calcite units

The desalination facility processes seawater from the Atlantic Ocean, with its concentration detailed in Table 1. Water is extracted via submersible pumps from nine boreholes and transferred to a feed tank for storage. Subsequently, it is conveyed through feed pumps to undergo a pretreatment phase that initiates with three Multi-Media Filtration (MMF) units (Figure 2-a). This stage aims to purify the water by eliminating suspended particles, sediment, and specific contaminants. Each MMF unit employs multiple layers of filter media with varying grain sizes to effectively capture and retain particles at different stratifications, thereby enhancing the overall efficiency of the filtration process. Upon exiting the three MMF units, the water is treated with an antiscalant to inhibit the formation and deposition of scale on the reverse osmosis (RO) membranes. The treated water is then directed to five Nirobox containers, each containing:

• Three parallel cartridge filters of the Codeline Aquiline type (Figure 2-b) represent the final step of pre-treatment. These cartridge filters are critical in the pre-filtration process, as they effectively remove larger particles and impurities that could potentially damage or obstruct the delicate reverse osmosis (RO) membrane. They also capture sediments such as sand, silt, rust, and other visible particles, which may originate from various sources, including aging pipelines, municipal supply systems, or well water.

• A high-pressure pump of the Grundfos type, rated at a nominal power of 90 kW, generates the requisite high pressure to propel water through the semi-permeable membrane within the RO system. This pressure is vital for overcoming osmotic pressure and facilitating the movement of water molecules through the membrane while leaving contaminants and impurities behind.

• Ten pressure vessels are detailed in Table 4, each containing five LG Chem 440 ES RO membranes (see Table 2), which constitute the core of the RO system and are responsible for removing contaminants and impurities from the water. The treated water then bifurcates into two pathways: the permeate, or filtered water, and the concentrate, or rejected water.

• A pressure exchanger of the iSave 50 type, designed to recover energy from the concentrate stream and transfer it to the feed water, thereby reducing overall energy consumption. The specifications for the iSave 50 are detailed in Table 3.

Each Nirobox is equipped with a cleaning system (CIP) with a capacity of 100 m^3, which operates automatically

upon the cessation of Nirobox activity. This system is responsible for the automated cleaning of cartridge filters and pressure vessels when the Nirobox is offline. Figure 2-c illustrates the configuration of the Nirobox and the CIP unit.

Subsequently, the permeate water accumulated from the five Niroboxes proceeds to the post-treatment phase, where pH regulation and remineralization occur. Initially, sulfuric acid (H_2SO_4) is dosed into the water, followed by passage through two Calcite units (Figure 2-d). After this, sodium hydroxide (NaOH) and sodium hypochlorite (NaClO) are added. Once these treatments are completed, the water meets drinking water standards and is transferred to a large freshwater storage tank. Finally, the freshwater is pumped to the distribution station. Figure 3 provides a comprehensive overview of the entire system.

Table 1. Nouadhibou SWRO feed water specifications

Element	Ca^{2+}	Mg^{2+}	Na^{+}	K^{+}	HCO_3^{-}	SO_4^{2-}	Cl^{-}	T(°C)	pH	Turbidity
TDS(mg/L)	441	1,403	11,640	428	152.8	2,920	20,932	25.5	8.17	< 1

Table 2. LG Chem 440 ES membrane specifications

Product Specifications	
Surface	41 m²
Rejection ration	99.8%
Minimum Salt Rejection	99.6%
Operating Specifications	
Max. Applied pressure	82.7 bar
Max. Chlorine concentration	< 0.1 ppm
Max. Operating temperature	45 °C
pH Range, Continuous (Cleaning)	2-11 (2-13)
Max. Feedwater turbidity	1.0 NTU
Max. Feed flow	17 m^3/h
Max. Pressure drop (ΔP) for each element	(1.0 bar)

Table 3. PEX iSave 50 specifications

Parameter	Value
Max. differential pressure (HP out-HP in)	5 bar
Max. pressure HP out (Max. allowable working pressure, MAWP)	83 bar
Min. pressure HP out (min. allowable working pressure)	40 bar
Max. pressure LP in (MAWP)	5 bar
Min. pressure on HP in, intermittent	2 bar
Min. allowable working pressure, LP in	2 bar

Table 3. (cont.)

Parameter	Value
Differential pressure at max. Flow, (LP in-LP out)	0.53 bar
Speed	[525-650] rpm
Flow at min. speed, HP out, in	42 m^3/h
Flow at max. speed. HP out	52 m^3/h
Max. allowable working flow, LP in	57.2 m^3/h
Salinity increase in membranes with a 40% recovery rate at a balanced flow	2-3%
Motor Efficiency at max. speed at 60 bar	93.7%

Table 4. Pressure vessel specification

Parameter	Value
Manufacturer	BEL Vessels
Model	BEL8-S-1000
Maximum operating pressure	69 bar
Minimum operating pressure	1 bar
Maximum operating pressure	49 °C
Minimum operating temperature	0.5 °C

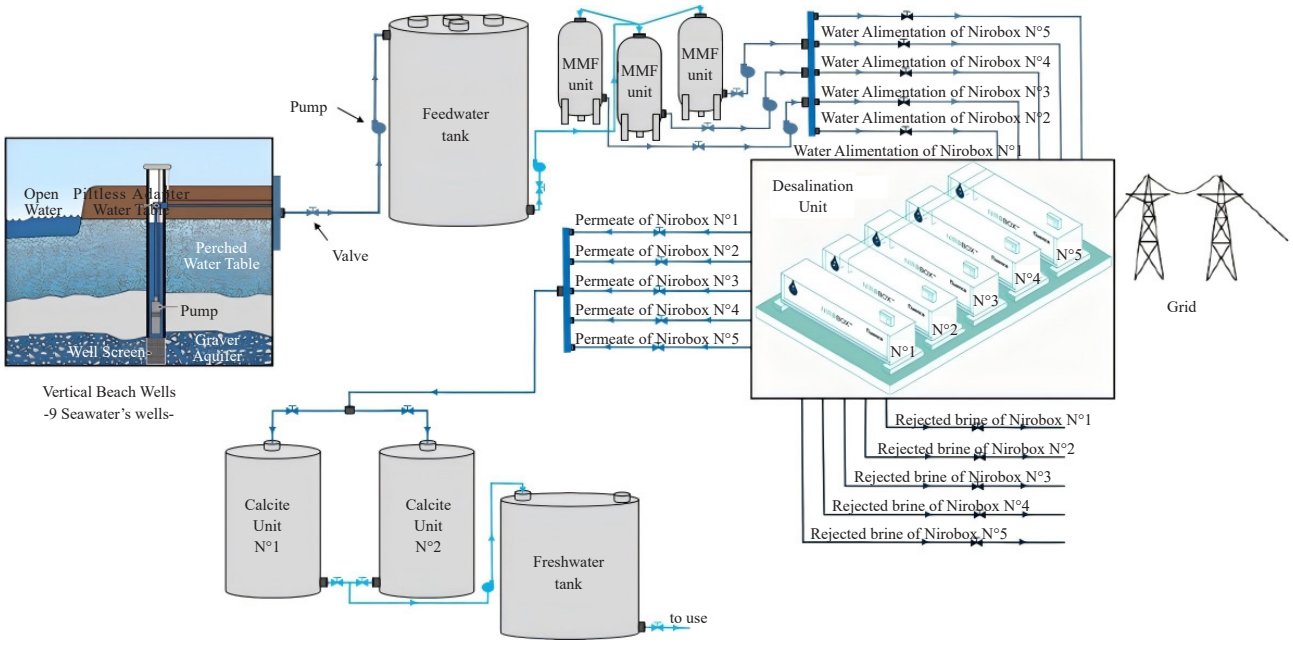

Figure 3. Schema of the Nouadhibou SWRO plant

4. Mathematical model of the system

Modeling is a procedure in which mathematical equations are used to describe real-life problems so as to solve these problems more easily [45]. Mathematical models are invaluable tools across numerous disciplines, offering a structured approach to understanding, analyzing, and predicting complex phenomena. The advent of digital computers in the mid-20th century revolutionized mathematical modeling, allowing for the simulation of intricate systems and the analysis of massive datasets. This led to the emergence of computational modeling as a powerful tool in scientific research and engineering. Mathematical modeling and optimization are critical components of the design process. They created remarkable results with the development in computer capabilities; due to this, several sophisticated software tools were developed that allow meshing, geometric modeling, and result presentation, in addition to sophisticated analytical algorithms [46]. Today, mathematical modeling is ubiquitous across various disciplines, from finance and healthcare to social sciences and environmental studies. Collaborative efforts between mathematicians, scientists, engineers, and policymakers continue to push the boundaries of modeling capabilities, driving innovation and discovery. Mathematical models offer precision, predictability, and insightful visualization of complex systems. They streamline analysis, optimize solutions, and facilitate interdisciplinary collaboration. Models enable risk assessment, adaptability, and effective communication of insights. Valuable for education and training, they are validated against empirical data, driving innovation and informing decision-making. Ultimately, mathematical models play a vital role in advancing understanding, informing policy, and fostering innovation across diverse fields.

In this work, the performance study of the desalination system was carried out by using the Matlab/Simulink software interface (see Figure 4). The objective of this work is to investigate the functionality and production performance of the reverse osmosis units by analyzing the importance of the pressure exchanger in reverse osmosis systems and acting on the mixing rate of the feed water with the water flow delivered by the pressure exchanger (PEX).

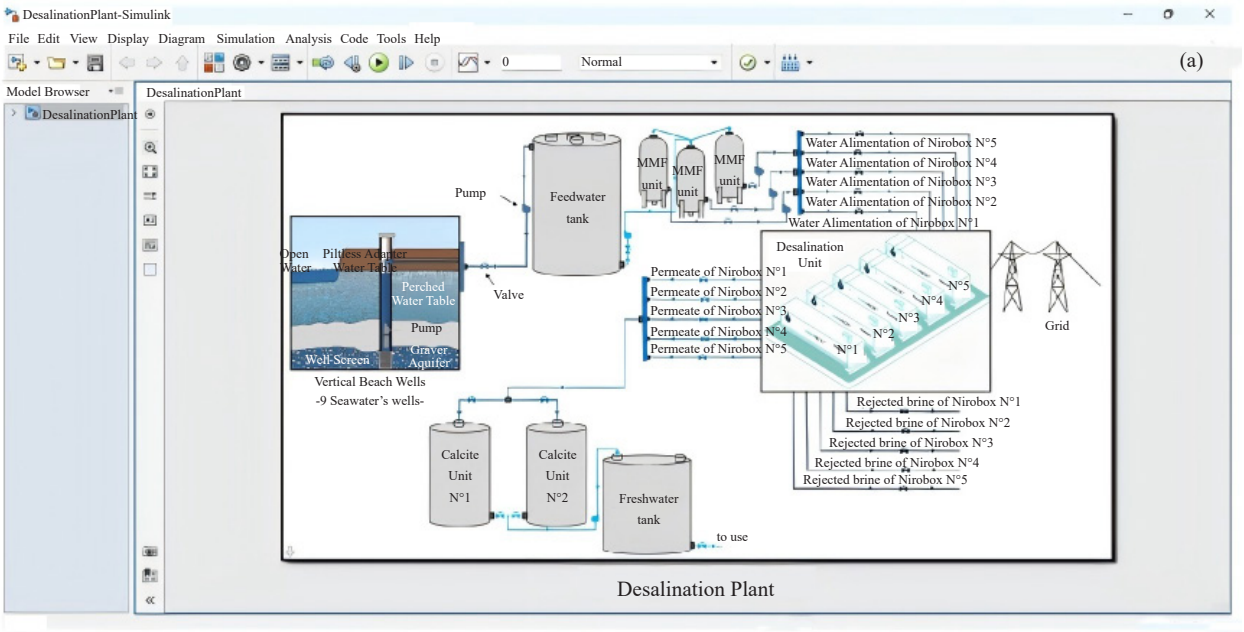

(b)

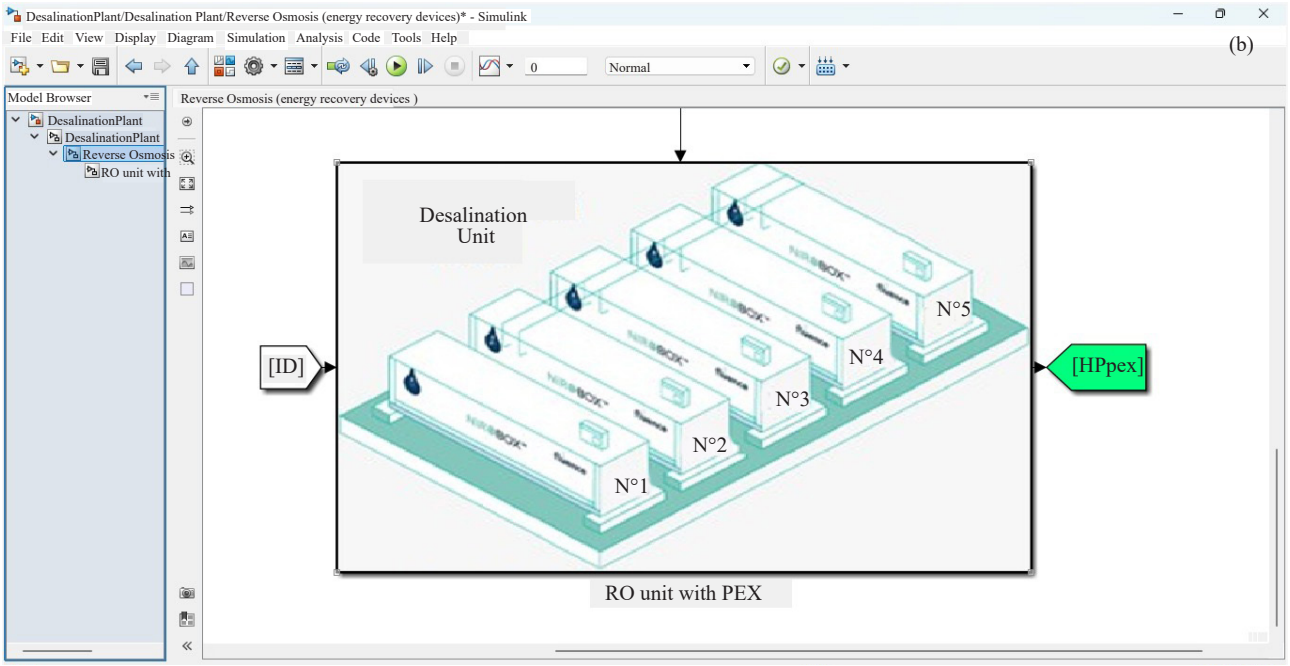
DesalinationPlant/Desalination Plant/Reverse Osmosis (energy recovery devices)* - Simulink
File Edit View Display Diagram Simulation Analysis Code Tools Help
Normal
Model Browser
DesalinationPlant
DesalinationPlant
Reverse Osmosis
RO unit with
Reverse Osmosis (energy recovery devices)
Desalination Unit
[ID]
N°1
N°2
N°3
N°4
N°5
[HPpex]
RO unit with PEX

(c)

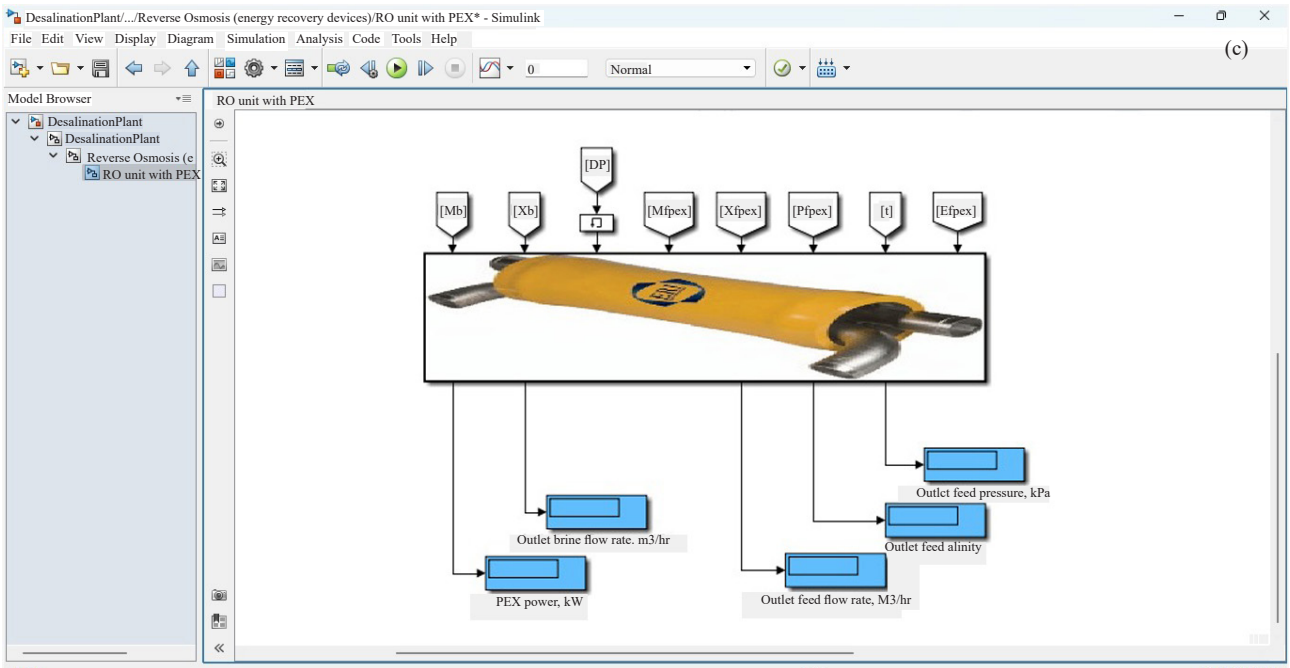
DesalinationPlant/.../Reverse Osmosis (energy recovery devices)/RO unit with PEX* - Simulink
File Edit View Display Diagram Simulation Analysis Code Tools Help
Normal
Model Browser
DesalinationPlant
DesalinationPlant
Reverse Osmosis (e
RO unit with PEX
RO unit with PEX
[DP]
[Mb]
[Xb]
[Mfpex]
[Xfpex]
[Pfpex]
[t]
[Efpex]
Outlet brine flow rate. m3/hr
PEX power, kW
Outlet feed flow rate, M3/hr
Outlet feed alinity
Outlet feed pressure, kPa

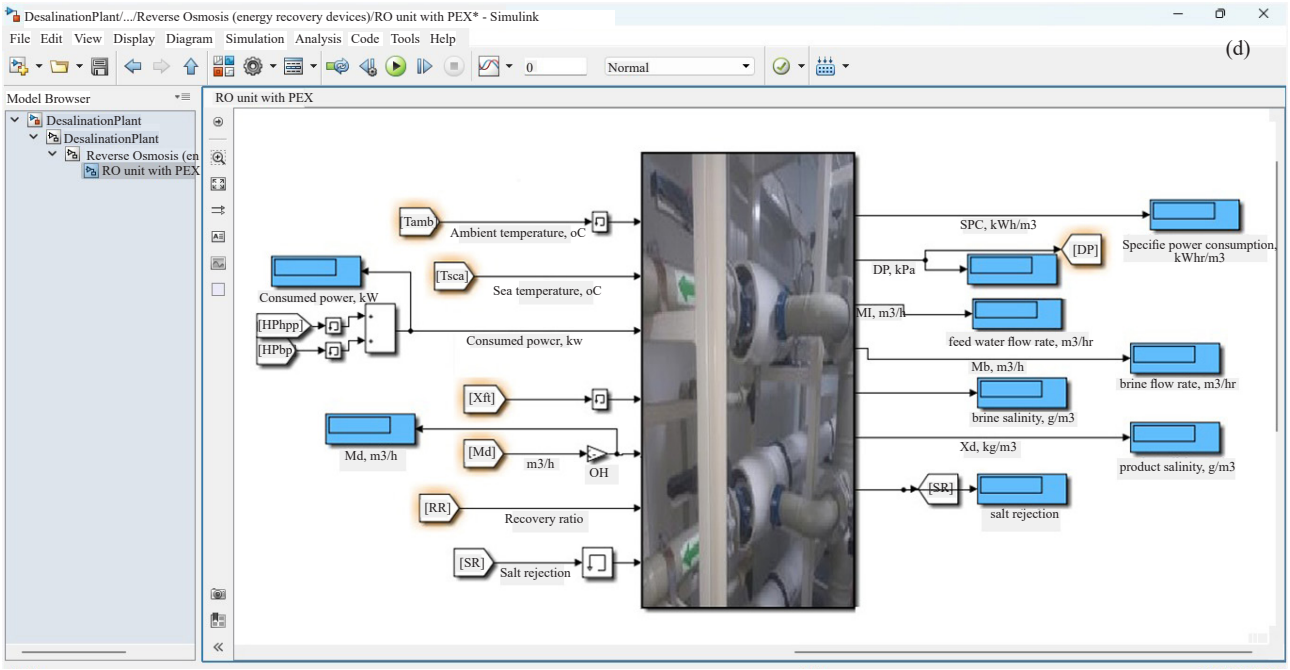

Figure 4. The system model browser under MATLAB/Simulink environment: (a) Desalination plant, (b) Desalination unit, (c) PEX unit, (d) RO unit

4.1 *Reverse osmosis mathematical model*

Reverse Osmosis modeling involves the use of mathematical and computational techniques to simulate and analyze the process of reverse osmosis, a widely used method for water purification and desalination. The RO system's behavior is simulated under various operating situations using a mathematical model, and performance metrics such as output water quality and pressure drop are predicted [6], [16].

RO modeling, if done properly, will result in fewer experiments needing to be undertaken, thereby reducing the time and costs associated with desalination [47]-[49]. Here are some key aspects to consider:

- Mathematical Modeling: Mathematical models of RO systems typically involve equations that describe fluid flow, mass transfer, and solute transport across the membrane. These models consider factors such as pressure, temperature, concentration, and membrane properties.

- Mass Balance Equations: Mass balance equations are fundamental to RO modeling. They describe the conservation of mass for water and solutes on both the feed side and the permeate side of the membrane.

- Transport Phenomena: Modeling RO requires an understanding of transport phenomena, including convective flow, diffusion, and solute rejection by the membrane. These phenomena influence the efficiency and performance of the RO system.

- Membrane Properties: The properties of the membrane, such as permeability, selectivity, and fouling resistance, are essential parameters in RO modeling. These properties affect the flux rate, salt rejection, and overall efficiency of the process.

- System Design and Optimization: RO modeling helps in the design and optimization of RO systems by predicting performance under different operating conditions. It allows engineers to optimize parameters such as pressure, flow rate, and membrane configuration to maximize efficiency and minimize energy consumption.

Pressure plays a fundamental role in the reverse osmosis filtration process. In this system, pressure is used to overcome the natural osmotic force and force water through the semi-permeable membrane. The pressure applied by the high-pressure pump is needed to compensate for osmotic pressure, which is the pressure exerted by dissolved solutes to prevent water from passing through the membrane. As a result, fresh water is produced through the application of high pressure on the supply side by the high-pressure motor pump according to the configuration of the RO membrane unit in addition to the quality and quantity of the production [2], [48].

The feed flow rate, kg/s is calculated based on the power load on the high-pressure pump (*HPP*, kW), the density (ρ), pump efficiency (η_p), and the pressure difference across the pump (ΔP) [6], [7], [16], [21], [49].

$$M_f = \frac{HPP \times \rho\left(T,\ X_f\right) \times \eta_p}{\Delta P} \tag{1}$$

The RO productivity, kg/s is then calculated based on the assigned recovery ratio (*RR*) as follows [6], [7], [16], [21], [49].

$$M_p = RR \times M_f \tag{2}$$

The product salt concentration X_p, g/kg is then calculated based on the feed salinity ratio X_f, g/kg and the salt rejection percentage *SR* (=~ 0.98) [6], [7], [16], [21], [49].

$$X_p = X_f \times (1 - SR) \tag{3}$$

The rejected brine kg/s is the difference between the feed flow rate and the product flow rate as follows [6], [7], [16], [21], [49].

$$M_b = M_f - M_p \tag{4}$$

Based on the mass and salt balances, the rejected salt concentration g/kg is then calculated [6], [7], [16], [21], [49].

$$X_b = \frac{M_f \times X_f - M_p \times X_p}{M_b} \tag{5}$$

The average salt concentration kg/m^3: [6], [7], [16], [21], [49].

$$X_{av} = \frac{M_f \times X_f + M_b \times X_b}{M_f + M_b} \tag{6}$$

The temperature correction factor, °C: [6], [7], [16], [21], [49].

$$TCF = exp\left(2,700 \times \left(\frac{1}{T + 273} - \frac{1}{298}\right)\right) \tag{7}$$

The membrane water permeability, k_W: [6], [7], [16], [21], [49].

$$k_W = 6.84 \times 10^{-8} \times \frac{18.6865 - 0.177 \times X_b}{T + 273} \tag{8}$$

The salt permeability k_s is [6], [7], [16], [21], [49].

$$k_s = FF \times TCF \times 4.72 \times 10^{-7} \times \left(0.06201 - \left(5.31 \times 10^{-5} \times (T + 273)\right)\right) \tag{9}$$

Where *FF* is the membrane-fouling factor (*FF* = 0.775). The calculations of osmotic pressure for the feed side (Π_f), brine side (Π_b), and distillate product side (Π_d) are found as follows [6], [7], [16], [21], [49]:

$$\Pi_f = 75.84 \times X_f \tag{10}$$

$$\Pi_b = 75.84 \times X_b \tag{11}$$

$$\Pi_d = 75.84 \times X_d \tag{12}$$

The average osmotic pressure on the feed side [6], [7], [16], [21], [49]:

$$\Pi_{av} = 0.5 \times (\Pi_f + \Pi_b) \tag{13}$$

The net osmotic pressure across the membrane [6], [7], [16], [21], [49]:

$$\Delta\Pi = \Pi_{av} - \Pi_d \tag{14}$$

The net pressure difference across the membrane [6], [7], [16], [21], [49]:

$$\Delta P = \left(\frac{M_d}{3,600 \times TCF \times FF \times A_e \times n_e \times N_v \times k_w} \right) + \Delta\Pi \tag{15}$$

Where A_e is the element area in m^2, n_e is the number of membrane elements, and N_v is the number of pressure vessels.

The specific power consumption (SPC, kWh/m^3) is then calculated based on the high-pressure pump (HPP, kW) and the product flow rate (M_p) [6], [7], [16], [21], [49]:

$$SPC = \frac{1,000 \times HPP}{3,600 \times M_p} \tag{16}$$

4.2 *Mathematical model of the energy recovery device*

4.2.1 *Splitter unit [6], [7], [16], [21], [49]*

PEX outlet pressure, kPa:

$$P_{f,\,PEX} = P_O = P_{f,\,RO} \tag{17}$$

Where P_O is the outlet pressure from the *HPP* and $P_{f,\,RO}$ is the inlet pressure in the pressure vessels.

Pressure exchanger unit feed flow rate (m^3/hr):

$$M_{f,\,PEX} = \eta_{PEX} \times M_{f,\,t} \tag{18}$$

Split feed flow rate, m^3/hr:

$$M_{f,\,RO} = (1 - \eta_{PEX}) \times M_{f,\,t} \tag{19}$$

Pressure exchanger unit feed water salinity, kg/m^3:

$$X_{f,\,PEX} = X_f \times M_{f,\,PEX} \tag{20}$$

Split feed water salinity, kg/m^3:

$$X_{f,\,RO} = X_f \times M_{f,\,RO} \tag{21}$$

Where η_{PEX} is the *PEX* Splitter ratio, X_f is Feed water salinity, kg/m^3, and $M_{f,\,t}$ is Inlet feed flow rate, m^3/hr.

4.2.2 *HPP unit [6], [7], [16], [21], [49]*

Pump power (power required), kW:

$$HHP = \frac{1{,}000 \times M_f \left(\Delta P - P_{fi}\right)}{3{,}600 \times \rho_f \times \eta_{HP}} \tag{22}$$

Feed temperature, °C:

$$T_O = \frac{HHP}{M_f \times C_p \times \eta_{HP}} + T_i \tag{23}$$

Where M_f is the *HPP* unit feed flow rate, m^3/hr, ρ_f is the feed density, P_{fi} is the *HPP* inlet pressure, η_{HP} is the efficiency of the high-pressure pump, and C_p is the specific heat capacity.

4.2.3 *Mixer unit [6], [7], [16], [21], [49]*

Mixer unit total flow rate salinity, g/m^3 is:

$$X_{f,\,t} = \frac{M_{f,\,spl} \times X_{f,\,spl} + M_{f,\,bp} \times X_{f,\,bp}}{M_{f,\,t}} \tag{24}$$

Where $M_{f,\,spl}$ and $X_{f,\,spl}$ are the split feed flow and split feed salinity, respectively, and $M_{f,\,bp}$ and $X_{f,\,bp}$ are booster pump feed flow rate and booster pump feed salinity, respectively.

Mixer unit total flow rate, m^3/hr:

$$M_{f,\,t} = M_{f,\,spl} + M_{f,\,bp} \tag{25}$$

4.2.4 *Booster pump unit [6], [7], [16], [21], [49]*

Booster pump power, kW:

$$HP_{bp} = \frac{1{,}000 \times M_{f,\,o} \times \left(\Delta P - P_{fi}\right)}{3{,}600 \times \rho_f \times \eta_{bp}} \tag{26}$$

Where $M_{f,\,o}$ is Feed flow rate to the mixer, m^3/hr, P_{fi} is Inlet feed pressure, kPa, and η_{bp} is Booster pump efficiency.

4.2.5 *Pressure exchanger unit PEX [6], [7], [16], [21], [49]*

Outlet feed pressure P_{fo}, kPa is calculated as:

$$P_{fo} = \frac{\left(M_{bi} \times \left(\Delta P_{bi} - 275\right) + M_{fi} \times P_{fi}\right) \times \eta_{f,\,PEX} - M_{bo} \times P_{bo}}{M_{fo}} \tag{27}$$

Outlet brine salinity, g/m^3:

$$X_{bo} = X_{bi} - 0.03 \times X_{bi} \tag{28}$$

Outlet feed salinity:

$$X_{fo} = \frac{X_{fi} + 0.03 \times X_{fi}}{M_{fo}} \tag{29}$$

PEX power, kW:

$$HP_{PEX} = \frac{M_{bo} \times P_{bo} + M_{fo} \times P_{fo}}{3,600} \tag{30}$$

Where $M_{bo} = M_{bi}$ is Outlet brine flow rate, m^3/hr, $M_{fo} = M_{fi}$ is Outlet feed flow rate, m^3/hr, $T_o = T_i$ is Blow-down temperature, °C, $P_{bo} = P_{fi}$ is Outlet brine pressure, kPa, and $\eta_{f,\,PEX}$ is the pressure exchanger efficiency.

The density, kg/m^3, is calculated as presented in the following function. This equation is applicable in the salinity range of 0 to 160 g/kg and for temperatures from 10 °C to 180 °C [6], [7], [16], [21], [49]:

$$\rho_w = \left(0.5 \times a_0 + a_1 \times Y + a_2 \times \left(2 \times Y^2 - 1\right) + a_3 \times \left(4 \times Y^3 - 3 \times Y\right)\right) \times 1,000 \tag{31}$$

Where:

$$a_0 = 2.01611 + 0.115313 \times \sigma + 0.000326 \times \left(\left(2 \times \left(\sigma^2\right)\right) - 1\right)$$

$$a_1 = -0.0541 + 0.001571 \times \sigma + 0.000423 \times \left(\left(2 \times \left(\sigma^2\right)\right) - 1\right)$$

$$a_2 = -0.006124 + 0.00174 \times \sigma + 0.000009 \times \left(\left(2 \times \left(\sigma^2\right)\right) - 1\right)$$

$$a_3 = 0.000346 + 0.00008 \times \sigma + 0.000053 \times \left(\left(2 \times \left(\sigma^2\right)\right) - 1\right)$$

Specific heat capacity (J/kg·°C): the specific heat of water at constant pressure is [6], [7], [16], [21], [49]:

$$C_p = \frac{1}{1,000} \times \left(a_p + b_p \times T + c_p \times T^2 + d_p \times T^3\right) \tag{32}$$

Where:

$$a_p = 4,206.8 - 6.6197 \times X + 1.2288 \times 10^{-2} \times X^2$$

$$b_p = -1.1262 + 5.4178 \times 10^{-2} \times X - 2.2719 \times 10^{-4} \times X^2$$

$$c_p = 1.2026 \times 10^{-2} - 5.3566 \times 10^{-4} \times X + 1.8906 \times 10^{-6} \times X^2$$

$$d_p = 6.8774\times10^{-7} + 1.517\times10^{-6}\times X - 4.4268\times10^{-9}\times X^2$$

5. Results and validation

Table 5 presents a comparative analysis of experimental results and numerical data from a desalination system integrated with an energy recovery unit. The findings indicate that the supply pressure measured experimentally from the high-pressure pump (HPP) is 60 bar, closely aligning with the numerical value of 56.7 bar obtained from the Matlab/Simulink model. For the feed flow, the numerical model predicts a rate of 85 m^3/h, while the experimental measurement is 83.3 m^3/h, resulting in a negligible error of 0.02%, which is deemed acceptable. The concentrated flow, as observed in the numerical model, is calculated at 59.5 m^3/h, compared to an experimental value of 58.33 m^3/h, again yielding an error of 0.02%, which is also within acceptable limits. In terms of salinity for both permeate and concentrate, the numerical model demonstrates satisfactory results with a very low margin of error (0.02%) relative to the experimental outcomes of the desalination system. This comparative study clearly illustrates the efficiency and validity of the numerical model for the desalination unit coupled with the energy recovery unit in this investigation.

Table 5. Data results for the proposed model vs. the experimental data with the pressure exchanger unit (PEX)

	Matlab results	Experimental results
Assigned parameters		
Ambient temperature, °C	25	25
Seawater temperature, °C	20	20
Seawater salinity, kg/m^3	38	38
Number of pressure elements/vessel, -	5	5
Number of vessels, -	10	10
Element area, m^2	41	41
Total area, m^2	2,050	2,050
High-pressure pump efficiency, %	80	80
Recovery ratio, %	30	30
Feed splitter ratio, %	68	67
The performance data results for the RO system with PEX		
Specific power consumption, kWh/m^3	2.817	2.82
Pressure, kPa	5,669	6,350
Feed water flow rate, m^3/h	85	83.3
Brine flow rate, m^3/h	59.5	58.33
Brine salinity, kg/m^3	55.3	53.95
Product salinity, kg/m^3	0.2283	0.591
Salt rejection, %	99.41	98.44
Product water flow rate, m^3/h	25.5	25.5
Feed to the booster pump, m^3/h	57.8	56.9
Split flow rate by PEX unit, m^3/h	27.2	27.4

Figure 5 illustrates the performance results associated with varying the operational energy of the reverse osmosis (RO) unit for a single Nirobox, depicting the specific desalination energy as a function of Recovery Rate (%) and Nirobox productivity (m^3/d). As shown in Figure 5-a, the RO unit operating without a pressure exchanger exhibits significantly higher electrical consumption for filtration compared to the same RO desalination system when integrated with a pressure exchanger. This variation in electrical consumption is fundamentally influenced by both the Recovery Ratio and the productivity of the Nirobox. Specifically, an allowable increase to 800 m^3/d at a low recovery rate of 20% necessitates substantial desalination energy of 400 kW in the absence of a pressure recovery unit. Conversely, the RO system with a pressure exchanger (RO-PEX) requires desalination energy that does not exceed 100 kW, leading to a reduction of 75% in the station's energy costs. Furthermore, an increase in the recovery rate of the desalination membrane directly impacts the electricity consumption of the station, resulting in lower electrical expenses, particularly in the RO-PEX configuration, which operates at approximately 124 kW at a Recovery Ratio of 40% and Nirobox productivity of 800 m^3/d.

In the case of the system operating without an energy recovery device (Figure 5-b), the specific power consumption for desalination ranges from 6 to 14 kWh/m^3, with an average value of approximately 10 kWh/m^3, which represents a significantly high cost for station operations. Notably, when the recovery rate is low (20-25%), the specific power consumption increases with productivity, reaching elevated levels of 8 to 14 kWh/m^3. This necessitates the pump unit to operate at high pressure, resulting in considerable electrical consumption, as illustrated in Figure 5-a. For a constant productivity level (for example, 600 m^3/d), the specific power consumption varies depending on the recovery rate, which can be attributed to fluctuations in the flow rate of the feed water. In contrast, the system equipped with an energy recovery unit generally exhibits a marked reduction in specific power consumption. For instance, at a productivity level of 400 m^3/d and a recovery rate of 40%, the specific power consumption is reduced to 2.7 kWh/m^3, compared to 6 kWh/m^3 for the system without an energy recovery unit. Furthermore, at a productivity of 800 m^3/d and a recovery rate of 22%, the specific power consumption decreases to 5 kWh/m^3, down from 14.5 kWh/m^3 in the absence of an energy recovery device. These significant differences in specific power consumption clearly demonstrate the advantages of implementing an energy recovery device, particularly the pressure exchanger in this study, which substantially reduces the operational costs of the station. Consequently, a reduction of over 75% in specific power consumption during filtration has been recorded, indicating a highly favorable economic and energy efficiency outcome.

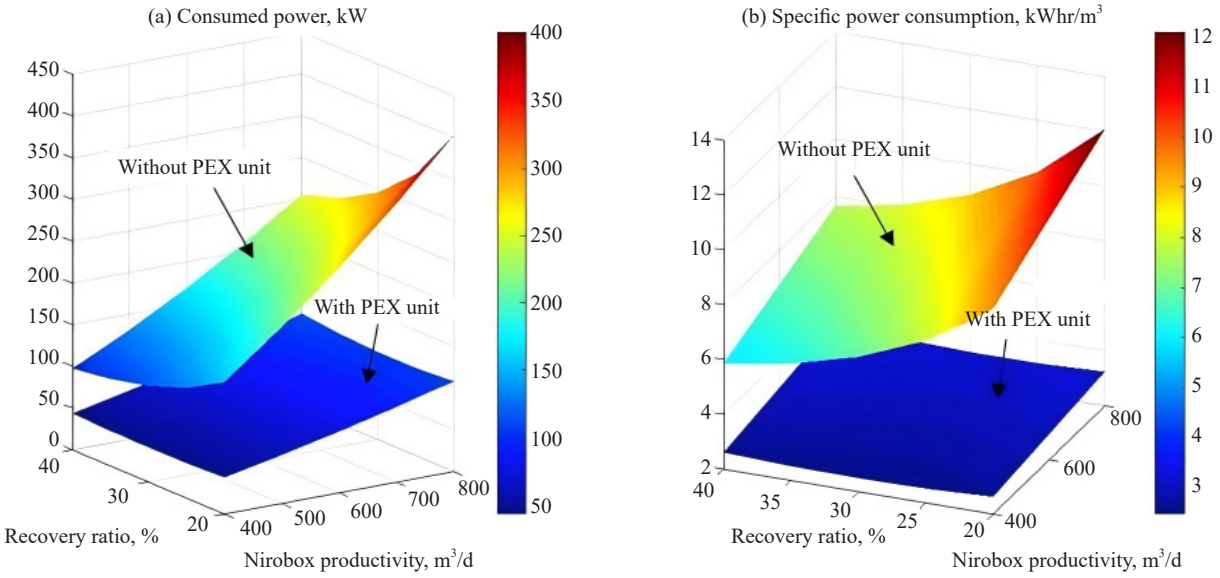

Figure 5. The Consumed power and SPC results of the RO unit for a single Nirobox with/without PEX unit

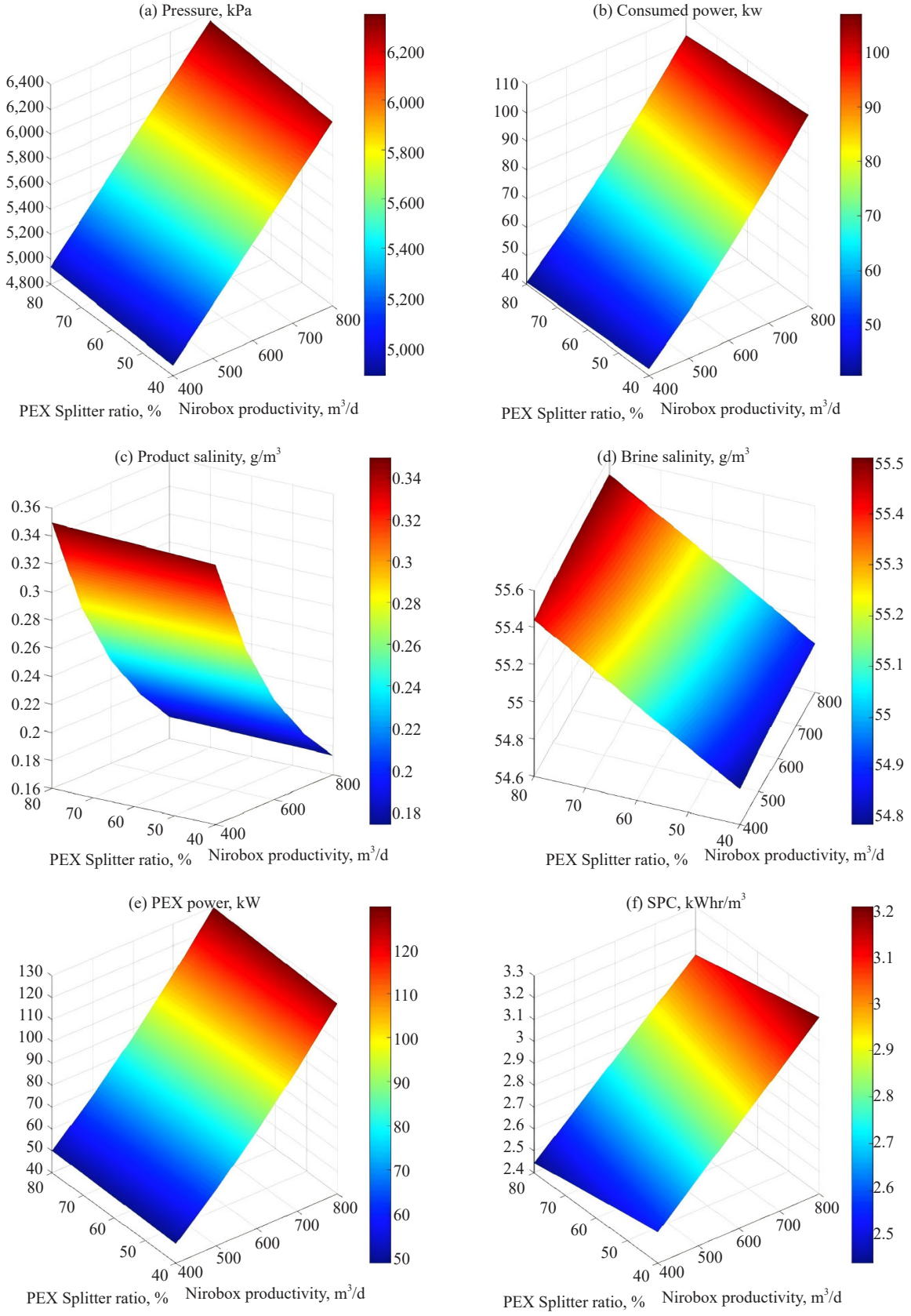

Figure 6. Performance results of a single Nirobox of the RO unit coupled with PEX unit

Figure 6 shows the performance results of a single Nirobox of the RO unit coupled with the pressure recovery unit as a function of daily desalination system productivity and the feed water distribution ratio. Figure 6-a shows clearly the variation effect of the feed water distribution ratio at the Pressure Exchanger level as well as the productivity of each Nirobox that is to say they influence the pressure applied to the reverse osmosis membranes and, it is absolutely remarkable that by increasing the feed water distribution ratio with an increase in productivity, the pressure of the system recognizes a very high value, that will block the pores of the membranes filtration, that cause an electricity consumption increase (Figure 6-b). In the case of productivity of 800 m^3/d, it is undeniable that the desalination unit has a high energy consumption of around ~110 kW when it is a PEX Splitter ratio of 40%, unlike when it is a PEX Splitter ratio of 80%, the power consumed is reduced to ~100 kW.

Regarding the quality of the water produced by the system, Figure 6-c demonstrates that variations in the PEX Splitter ratio of the pressure recovery unit have a minimal impact on the salinity of the permeate. In contrast, changes in system productivity exhibit a strong inverse correlation with permeate quality. Specifically, as productivity increases from 400 m^3/d to 800 m^3/d, the salinity of the permeate decreases from 0.35 g/m^3 to 0.18 g/m^3. As for the brine salinity (in g/m^3), Figure 6-d indicates that variations in desalination unit productivity have a negligible effect on brine salinity. However, when the PEX Splitter ratio is adjusted, there is a noticeable increase in brine salinity. Specifically, the brine salinity rises from 54.7 g/m^3 to 55.45 g/m^3 as the PEX Splitter ratio increases from 40% to 80%, respectively.

Figure 6-e illustrates the variation in power (kW) generated by the PEX unit as a function of both the desalination unit's productivity and the PEX Splitter ratio. Specifically, the system's productivity affects the power output; for instance, with a PEX Splitter ratio of 40%, the power delivered by the recovery unit ranges from approximately 45 kW at a productivity of 400 m^3/day to 127 kW at 800 m^3/day. Conversely, the PEX Splitter ratio has a minimal effect on the power generated by the PEX unit.

In Figure 6-f, the specific power consumption (SPC, kW/m^3) is depicted. Both the desalination unit's production level and the PEX Splitter ratio influence the SPC. Notably, the system's productivity has a substantial impact on the SPC-higher productivity results in a higher SPC. However, increasing the PEX Splitter ratio from 40% to 80% leads to a reduction in SPC, which is advantageous for economic optimization in the desalination industry.

Regarding the actual productivity of the station (600 m^3/day), with a PEX Splitter ratio of 64.5% and an operating efficiency of 30%, the system power output is measured at 60 kW, which is in close agreement with the real value of 58 kW. This demonstrates the accuracy of the numerical model at this operating point. Additionally, the specific power consumption (SPC) is calculated to be 3 kWh/m^3, which is reasonably close to the actual value of 2.47 kWh/m^3. However, the system pressure is calculated to be 54 bars, which is somewhat lower than the actual value of 63.2 bars. In terms of product salinity, the model predicts a value of 0.18 g/m^3, significantly lower than the real value of 0.75 g/m^3. Finally, the brine salinity is estimated to be 55.15 g/m^3.

6. Conclusion

This study aims to present the performance of the seawater desalination system, i.e., the reverse osmosis desalination system coupled with the pressure exchanger unit assisted by the local electricity network. Nouadhibou-Mauritania (North Africa) is the area studied in this work, a city that recognizes a very important water stress; on the other hand, they are characterized by a very important renewable energy potential. This study demonstrates the coupled desalination unit with the pressure exchanger energy recovery unit (RO-PEX) for a production of 400-800 m^3/d of freshwater. It is observed that the importance of the PEX unit, in particular the PEX Splitter ratio, directly influences the SPC of desalination and the overall economics of the installation.

The results show that the permeate salinity decreases from 0.35 g/m^3 to 0.18 g/m^3 during productivity from 400 m^3/d to 800 m^3/d. Also, with PEX, the specific power consumption is significantly reduced. For instance, at a productivity of 400 m^3/day and a recovery rate of 40%, the specific power consumption drops to 2.7 kWh/m^3, compared to 6 kWh/m^3 without the energy recovery unit. Concerning the PEX splitter ratio, it has a low impact on the PEX power showing a reduction of 9% in case of varying the PEX Splitter from 40 to 80% at 800 m^3/d of productivity. These important differences observed in both examples show perfectly well the benefit of implementing an energy recovery, particularly the PEX. However, the energy factor of desalination is still high, which requires a reduction by optimizing the

desalination system and integrating renewable energy sources that will be the subject of the next work.

Conflict of interest

The authors declare no conflict of interest.

References

[1] B. Huang, K. Pu, P. Wu, D. Wu, and J. Leng, "Design, selection and application of energy recovery device in seawater desalination: A review," *Energies*, vol. 13, no. 16, pp. 4150, 2020.

[2] S. Tianbao, L. Lu, B. Jianwei, X. Xidong, Y. Yulian, and P. Chunyou, "Key points of design and equipment selection of reverse osmosis seawater desalination high-pressure system," *Water Purification Technology*, vol. 38, pp. 131-134, 2019.

[3] I. C. Escobar and A. Schäfer, *Sustainable Water for the Future: Water Recycling Versus Desalination*. Amsterdam: Elsevier, 2009.

[4] M. A. Thompson, "An integrated approach to scale up the market penetration of low carbon technologies in developing countries and water scarce regions," Ph. D. dissertation, University of California, Los Angeles, Los Angeles, California, United States, 2016. Available: https://escholarship.org/uc/item/9vb98257. [Accessed: November 3rd, 2024].

[5] W. Peng, A. Maleki, M. A. Rosen, and P. Azarikhah, "Optimization of a hybrid system for solar-wind-based water desalination by reverse osmosis: Comparison of approaches," *Desalination*, vol. 442, pp. 16-31, 2018.

[6] A. Lilane, D. Saifaoui, S. Ettami, M. Chouiekh, Y. Aroussy, and M. A. S. Eldean, "Modeling and simulation of solar chimney/HWT power plant for the assistance of reverse osmosis desalination and electric power generation," *Desalination Water Treatment*, vol. 286, pp. 1-15, 2023.

[7] A. Lilane, D. Saifaoui, S. Hariss, H. Jenkal, and M. Chouiekh, "Modeling and simulation of the performances of the reverse osmosis membrane," *Materials Today Proceedings*, vol. 24, pp. 114-118, 2020.

[8] N. AlZainati, H. Saleem, A. Altaee, S. J. Zaidi, M. Mohsen, A. Hawari, and G. J. Millar, "Pressure retarded osmosis: Advancement, challenges and potential," *Journal of Water Process Engineering*, vol. 40, pp. 101950, 2021.

[9] Z. M. Ghazi, S. W. F. Rizvi, W. M. Shahid, A. M. Abdulhameed, H. Saleem, and S. J. Zaidi, "An overview of water desalination systems integrated with renewable energy sources," *Desalination*, vol. 542, pp. 116063, 2022.

[10] S. J. Zaidi and H. Saleem, *Reverse Osmosis Systems: Design, Optimization and Troubleshooting Guide*. Amsterdam: Elsevier, 2021.

[11] B. Schneider, "Selection, operation and control of a work exchanger energy recovery system based on the Singapore project," *Desalination*, vol. 184, no. 1-3, pp. 197-210, 2005.

[12] A. Zhu, P. D. Christofides, and Y. Cohen, "Effect of thermodynamic restriction on energy cost optimization of ro membrane water desalination," *Industrial & Engineering Chemistry Research*, vol. 48, no. 13, pp. 6010-6021, 2009. Available: https://doi.org/10.1021/ie800735q.

[13] A. Zhu, P. D. Christofides, and Y. Cohen, "Energy consumption optimization of reverse osmosis membrane water desalination subject to feed salinity fluctuation," *Industrial & Engineering Chemistry Research*, vol. 48, no. 21, pp. 9581-9589, 2009.

[14] Z. Zimerman, "Development of large capacity high efficiency mechanical vapor compression (MVC) units," *Desalination*, vol. 96, no. 1-3, pp. 51-58, 1994.

[15] A. Al-Karaghouli and L. L. Kazmerski, "Energy consumption and water production cost of conventional and renewable-energy-powered desalination processes," *Renewable and Sustainable Energy Reviews*, vol. 24, pp. 343-356, 2013.

[16] A. Lilane, D. Saifaoui, Y. Aroussy, M. Chouiekh, M. S. Eldean, and A. Mabrouk, "Simulation and optimization of pilot reverse osmosis desalination plant powered by photovoltaic solar energy," *Desalination Water Treatment*, vol. 258, pp. 16-42, 2022.

[17] R. L. Stover, "SWRO process simulator," *Desalination*, vol. 221, no. 1-3, pp. 126-135, 2008.

[18] A. Al-Qaraghuli and L. L. Kazmerski, "Comparisons of technical and economic performance of the main desalination processes with and without renewable energy coupling," National Renewable Energy Lab. (NREL), Golden, CO (United States), Tech. Report. NREL/CP-5900-54735, 1 Jan. 2012. Available: https://www.osti.gov/

biblio/1056119. [Accessed: November 3rd, 2024].
[19] R. L. Stover, "Seawater reverse osmosis with isobaric energy recovery devices," *Desalination*, vol. 203, no. 1-3, pp. 168-175, 2007.
[20] M. Kettani and P. Bandelier, "Techno-economic assessment of solar energy coupling with large-scale desalination plant: The case of Morocco," *Desalination*, vol. 494, pp. 114627, 2020.
[21] A. Lilane, D. Saifaoui, S. Ettami, M. Chouiekh, and Y. Aroussy, "Simulation and optimization of a RO/EV pilot reverse osmosis desalination plant powered by PV solar energy: the application to brackish water at low concentration," *The European Physical Journal Applied Physics*, vol. 97, pp. 82, 2022.
[22] R. L. Stover, "Energy recovery device performance analysis," *Water Middle East*, 2005.
[23] A. Cipollina, G. Micale, and L. Rizzuti, "A critical assessment of desalination operations in Sicily," *Desalination*, vol. 182, no. 1-3, pp. 1-12, 2005.
[24] E. Jones, M. Qadir, M. T. van Vliet, V. Smakhtin, and S. Kang, "The state of desalination and brine production: A global outlook," *Science of the Total Environment*, vol. 657, pp. 1343-1356, 2019.
[25] N. M. Eshoul, B. Agnew, M. A. Al-Weshahi, and M. S. Atab, "Exergy analysis of a two-pass reverse osmosis (RO) desalination unit with and without an energy recovery turbine (ERT) and pressure exchanger (PX)," *Energies*, vol. 8, no. 7, pp. 6910-6925, 2015.
[26] C. Wang, S. Wang, K. Wang, Y. Xiao, Q. Ma, D. Song, R. Wang, and Y. Zhang, "Developmental impediment and prospective trends of desalination energy recovery device," *Desalination*, vol. 578, pp. 117465, 2024.
[27] T. M. Mansour, T. M. Ismail, K. Ramzy, and M. Abd El-Salam, "Energy recovery system in small reverse osmosis desalination plant: Experimental and theoretical investigations," *Alexandria Engineering Journal*, vol. 59, no. 5, pp. 3741-3753, 2020.
[28] J. S. Kim, J. Chen, and H. E. Garcia, "Modeling, control, and dynamic performance analysis of a reverse osmosis desalination plant integrated within hybrid energy systems," *Energy*, vol. 112, pp. 52-66, 2016.
[29] T. M. Missimer, N. Ghaffour, A. H. Dehwah, R. Rachman, R. G. Maliva, and G. Amy, "Subsurface intakes for seawater reverse osmosis facilities: Capacity limitation, water quality improvement, and economics," *Desalination*, vol. 322, pp. 37-51, 2013.
[30] K. Quteishat and M. Abu-Arabi, "Promotion of solar desalination in the MENA region," *Middle East Desalination Research Center*. 2006.
[31] A. J. Schunke, G. A. Hernandez Herrera, L. Padhye, and T.-A. Berry, "Energy recovery in SWRO desalination: current status and new possibilities," *Frontiers in Sustainable Cities*, vol. 2, pp. 9, 2020.
[32] M. J. Guirguis, "Energy recovery devices in seawater reverse osmosis desalination plants with emphasis on efficiency and economical analysis of isobaric versus centrifugal devices," M.S. thesis, University of South Florida, Florida, USA, 2011. Available: https://digitalcommons.usf.edu/etd/3135/. [Accessed: November 3rd, 2024].
[33] F. Egli, B. Steffen, and T. S. Schmidt, "Bias in energy system models with uniform cost of capital assumption," *Nature Communications*, vol. 10, no. 1, pp. 4588, 2019.
[34] M. Hunter, G. Ofosu-Peasah, T. W. Anti, E. T. Akonor, R. E. Ghastalany, and G. Moberg, "Learnings from West Africa's regional experiences in the gold sector," *Globalinitiative.net*, 2023. [Online]. Available: https://globalinitiative.net/analysis/learning-from-west-africas-regional-experiences-in-the-gold-sector/. [Accessed: November 3rd, 2024].
[35] A. Ruiz-García, I. Nuez, and M. Khayet, "Performance assessment and modeling of an SWRO pilot plant with an energy recovery device under variable operating conditions," *Desalination*, vol. 555, pp. 116523, 2023.
[36] S. Hong, K. Park, J. Kim, A. B. Alayande, and Y. Kim, *Seawater Reverse Osmosis (SWRO) Desalination: Energy Consumption in Plants, Advanced Low-Energy Technologies, and Future Developments for Improving Energy Efficiency*. London: IWA Publishing, 2023.
[37] M. Mohammed, M. El Aoud Mohamed, and M. F. Zahra, "Solving the energy consumption barrier in brackish water reverse osmosis desalination plants: A genetic algorithm and energy recovery approach," *Advances in Systems Science and Applications*, vol. 24, no. 2, pp. 203-218, 2024.
[38] P. S. Bhambare, M. C. Majumder, and C. V. Sudhir, "Solar thermal desalination: a sustainable alternative for Sultanate of Oman," *International Journal of Renewable Energy Research*, vol. 8, no. 2, pp. 733-751, 2018.
[39] F. E. Ahmed, R. Hashaikeh, A. Diabat, and N. Hilal, "Mathematical and optimization modelling in desalination: State-of-the-art and future direction," *Desalination*, vol. 469, pp. 114092, 2019.
[40] W. L. Ang and A. W. Mohammad, "Mathematical modeling of membrane operations for water treatment," in *Advances in Membrane Technologies for Water Treatment*, Amsterdam: Elsevier, 2015, pp. 379-407.
[41] G. P. Narayan, R. K. McGovern, and S. M. Zubair, "High-temperature-steam-driven, varied-pressure,

humidification-dehumidification system coupled with reverse osmosis for energy-efficient seawater desalination," *Energy*, vol. 37, no. 1, pp. 482-493, 2012.
[42] M. Li, "Reducing specific energy consumption in Reverse Osmosis (RO) water desalination: An analysis from first principles," *Desalination*, vol. 276, no. 1-3, pp. 128-135, 2011.
[43] D. J. Woodcock and I. M. White, "The application of pelton type impulse turbines for energy recovery on sea water reverse osmosis systems," *Desalination*, vol. 39, pp. 447-458, 1981.
[44] A. A. Ahuchaogu, O. J. Chukwu, A. I. Obike, C. E. Igara, I. C. Nnorom, and J. B. O. Echeme, "Reverse osmosis technology, its applications and nano-enabled membrane," *International Journal of Advanced Research in Chemical Science*, vol. 5, no. 2, pp. 20-26, 2018.
[45] B. D. Negewo, "Renewable energy desalination: an emerging solution to close the water gap in the Middle East and North Africa." *World Bank Publications*, 2012.
[46] H. A. Maddah, A. S. Alzhrani, A. M. Almalki, M. Bassyouni, M. H. Abdel-Aziz, M. Zoromba, and M. A. Shihon, "Determination of the treatment efficiency of different commercial membrane modules for the treatment of groundwater," *Journal of Materials and Environmental Sciences*, vol. 8, no. 6, pp. 2006-2012, 2017.
[47] A. Mengesha and O. Sahu, "Sustainability of membrane separation technology on groundwater reverse osmosis process," *Cleaner Engineering and Technology*, vol. 7, pp. 100457, 2022.
[48] A. Dang, J. M. Bennett, A. Marchuk, S. Marchuk, A. J. W. Biggs, and S. R. Raine, "Validating laboratory assessment of threshold electrolyte concentration for fields irrigated with marginal quality saline-sodic water," *Agricultural Water Management*, vol. 205, pp. 21-29, 2018.
[49] M. A. Sharaf, "Thermo-economic comparisons of different types of solar desalination processes," *Journal of Solar Energy Engineering*, vol. 134, no. 3, pp. 031001, 2012.